Tidal stream energy in the Netherlands—Resource assessment and future effects due to mean sea level rise

Bolhuis, Sijbrand; Alday Gonzalez, M.F.; Lavidas, George

DOI
10.1016/j.renene.2025.124214

Publication date
2025

Document Version
Final published version

Published in
Renewable Energy

Renewable Energy 256 (2026) 124214

Contents lists available at ScienceDirect

Renewable Energy

journal homepage: www.elsevier.com/locate/renene

Tidal stream energy in the Netherlands—Resource assessment and future effects due to mean sea level rise

Sijbrand Bolhuis *, Matias Alday, George Lavidas

Marine Renewable Energies Lab, Department of Hydraulic Engineering, Faculty of Civil Engineering and Geosciences, Delft University of Technology, Stevinweg 1, Delft, 2628 CN, Zuid Holland, Netherlands

A R T I C L E I N F O

Keywords:
Tidal stream energy
Tidal resource
Tidal modelling
Sea-level rise
Netherlands

A B S T R A C T

In line with the global shift to transition away from fossil fuels to sustainable energy sources, tidal stream energy has emerged as a promising renewable option. This study investigates the tidal stream energy resources along the Dutch coast and focuses on the impact of Mean Sea Level (MSL) rise on the future resource potential. A THETIS high-resolution unstructured model is used. The model is validated against sea surface elevations, and the Dutch tidal stream resource uncertainties are well defined. The validated model is used to evaluate the tidal stream energy potential of the Netherlands, regions in the Wadden Sea and Westerschelde in Zeeland display noteworthy potential, evidenced by maximum average flow velocities of 1.3 m/s and maximum average energy densities of 1600 W/m^2 for the Wadden Sea and maximum average flow velocities of 0.75 m/s and maximum average energy densities of 300 W/m^2 for the Westerschelde. Forecasting the 2050 tidal stream resource, considering a projected 118 mm MSL rise, results indicate persistent energy characteristics, with minimal fluctuations in average velocities and average energy density when compared to the 2016 model. In the Wadden Sea and Zeeland, respectively, only marginal changes of +25 W/m^2, and +8 W/m^2 are observed in average energy density for those same locations. Furthermore, the inclusion of long-term constituents has negligible effects on the 2050 results, emphasising the stability of the tidal stream energy source. Tidal stream energy in the Netherlands stands out as a reliable and resilient energy source, demonstrating consistency in the face of projected MSL rise. Such predictability has the potential to contribute significantly to fostering a sustainable and secure energy system in the Netherlands, while aligning with global efforts to combat climate change.

1. Introduction

As the world seeks to transition away from fossil fuels and embrace sustainable energy sources, tidal stream energy has emerged as a promising renewable option, especially because of its highly predictable nature. In Europe, highest level of tidal energy resources are found in the territorial waters of the United Kingdom (UK) [1]. However, tidal energy, can be of major importance even at lower energy sites. The predictable and site specificity of the stream tidal resource, can assist in the decarbonisation of specific regions [2]. UK's high potential sites like Pentland Firth and Orkney Waters at the North of Scotland [3] and Bristol Channel between South Wales and Southwest England [4], have been thoroughly investigated on its resources. Similarly, research efforts have been undertaken globally in promising locations like France [5], United States of America (USA) and Canada [6], China [7], Australia [8] and Indonesia [9]. A UK study by Coles et al. (2021) [10] has shown the potential of meeting at least 11% of the UK electricity demand using tidal stream energy solutions.

However, a notable lack of research in quantification of the tidal stream resources is found for the Dutch coastlines. Historically, the tidal research focus within the Netherlands has centred on topics such as tidal sediment transport, particularly in the Wadden Sea [11], tidal behaviour, with studies showing Sea Level Rise (SLR)-induced increases in tidal amplitudes for example [12], and the exploration of tidal barrages, including analyses on hydraulic and environmental impacts, as well as assessments of tidal energy production in the Oosterschelde [13] with different types of technologies as tidal stream and potential larger structures such as hydrodynamic barriers [14].

The most recent attempt to evaluate the resource tidal stream potential was conducted by Alday and Lavidas (2024) [15]. The study found a moderate potential for tidal streams energy along the Dutch coast, with the most promising sites identified in Zeeland and the Wadden Sea. In addition, a critical gap exists regarding the impact of climate change effects on this resource potential. The Netherlands, with its

* Corresponding author.
E-mail addresses: S.P.Bolhuis@tudelft.nl, sijbrandbolhuis@gmail.com (S. Bolhuis).

https://doi.org/10.1016/j.renene.2025.124214
Received 23 January 2024; Received in revised form 8 August 2025; Accepted 8 August 2025
Available online 8 September 2025

expansive coastline and shallow coastal areas in the Wadden Sea and Zeeland, is significantly vulnerable to the impacts of Mean Sea Level (MSL) rise [16]. Given the global evidence suggesting adjustments in tidal behaviour due to MSL rise [17,18], it becomes imperative to investigate and address how such changes may impact Dutch tidal stream resources. This paper seeks to fill this gap by examining the potential effects of MSL rise on the tidal stream resources along the Dutch coast.

This study for the first time evaluates and quantifies the impact of MSL on the Dutch tidal stream resource by employing a distinct methodology, incorporating the impact of Climate Change to assess and enhance the understanding of Dutch tidal stream potential. The resulted forecast of tidal stream energy flux, complements the hindcast of Alday and Lavidas (2024) [15] and uncovers the untapped tidal stream resource in the Netherlands that is often overlooked. Understanding the potential changes and challenges associated with tidal stream energy due to climate change is crucial for ensuring a sustainable and secure energy system in the Netherlands and aligning with global efforts to combat climate change. By comprehensively assessing the impact MSL rise on tidal stream resources, this study enables decision-makers to evaluate the future energy security offered by tidal stream energy, and make well-informed choices regarding the implementation of potential tidal stream energy sites.

In this paper, Section 2 presents the hydrodynamic model setup, validation, the Mean Sea Level (MSL) scenario analysis and the model-runs setup. Section 3 presents results and discussion, analysing the observed model outcomes. Section 4 provides comprehensive conclusions on the course of tidal stream resources given MSL rise along the Dutch coast by 2050.

2. Materials & methods

2.1. Tidal model and set up

Tidal simulation is done using open ocean model THETIS [19], which has proved itself for applications in tidal simulation for coastal regions [10,20,21]. Leveraging the Firedrake finite element framework [22] and PETSc [23], THETIS discretises and solves the Partial Differential Equations (PDE) governing the 2D nonlinear shallow water wave equations over an unstructured mesh. The system undergoes spatial and temporal resolution, utilising a CG-type method [24] for spatial discretisation and a 2-stage 2nd order L-stable Diagonally Implicit Runge Kutta method, DIRK22, for implicit temporal evolution with a constant time step of 300 s [25]. The depth-averaged shallow water equations within the computational framework of THETIS are hereby articulated as follows:

$$\frac{\partial \eta}{\partial t} + \nabla \cdot \left(H_d \mathbf{u} \right) = 0 \tag{1}$$

$$\frac{\partial \mathbf{u}}{\partial t} + \mathbf{u} \cdot \nabla \mathbf{u} - \upsilon \nabla^2 \mathbf{u} + f \mathbf{u}^{\perp} + g \nabla \eta = -\frac{\tau_b}{\rho H_d} \tag{2}$$

where η (m) is the free surface water elevation, $\mathrm{H_d}$ (m) is the total water depth ($\eta + h$), ν ($\mathrm{m^2\ s^{-1}}$) is the kinematic viscosity, u ($\mathrm{m\ s^{-1}}$) is the depth-averaged velocity vector, $f\mathbf{u}^{\perp}$ represents the Coriolis effect (calculated using $f = 2 * \omega * sin(latitude * \pi/180)$), and τ_b ($\mathrm{kg\ m^{-1}\ s^{-2}}$) is the Bed shear stress. The influence of bed shear stress (τ_b) is modelled using the formulation of Manning's n, defined as:

$$\frac{\tau_b}{\rho} = g n^2 \frac{|\mathbf{u}|\mathbf{u}}{H_d^{\frac{1}{3}}} \tag{3}$$

In which ρ ($\mathrm{kg\ m^{-3}}$) is the density of the water and g ($\mathrm{m\ s^{-2}}$) is gravitational acceleration. The base model's Manning value, quantifying the loss of energy in open channels due to bottom friction, is set at 0.035 [–]. Wetting and drying is not taken into account, simplifying computations in exposed areas. Numerical stability is maintained by enforcing a minimum depth of 7.5 m over the domain. Model viscosity is set at 1.0 [N s/$\mathrm{m^2}$] and all models make use of a sponge layer of high drag and high viscosity at the forced open ocean boundary, a method that has been used before by Mawson 2022 [26]. Tidal forcing is applied at the open ocean boundary, using the TPXO tidal dataset by Egbert & Erofeeva, 2002 [27] from which 8 main constituents (M2, S2, K1, O1, P1, Q1, N2, K2) were used.

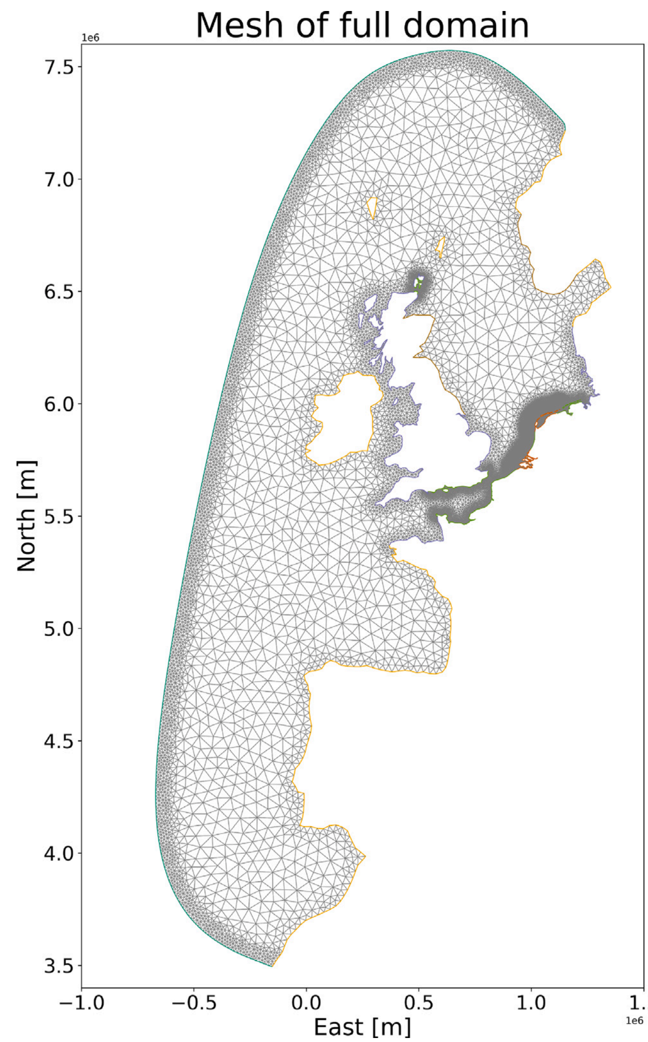

Fig. 1. North Atlantic and high-fidelity regions mesh created with qmesh, containing 65k nodes and 128k elements, with 500 m resolution at the Netherlands coastlines.

2.2. Mesh construction

To ensure accurate modelling of tidal waves at the Dutch coast, the open ocean boundary is positioned at larger depths well outside the shelf break, to apply boundary conditions in a quiet see state and mitigate bottom friction effects on developing waves and thereby enhance accuracy, resulting in a large domain that requires an unstructured grid for computational feasibility. The unstructured mesh was generated using qmesh [28] and gmsh [29], incorporating high-resolution coastline data (∼1.85 km resolution) from GSHHG [30] and was post-processed in QGIS [31].

The mesh shown in Fig. 1, was constructed in UTM30 (Universal Transverse Mercator coordinate system), using 6 distinct resolutions spans, from which the 500 m resolution was the highest density, applied in the Wadden Sea and along the coastline in Zeeland.

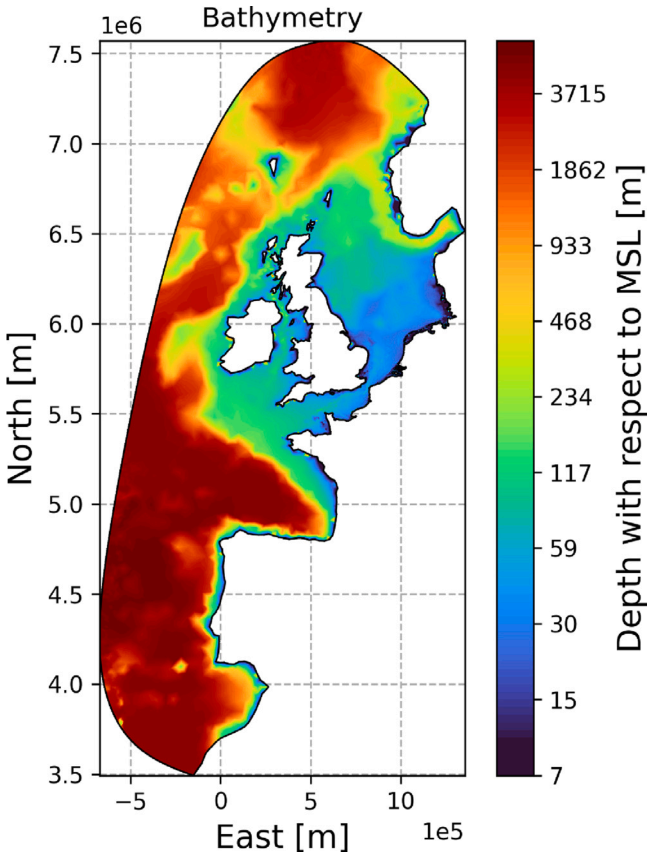

Fig. 2. Bathymetry of the domain in meters with regards to mean sea level as provided by EMODnet [32].

Bathymetric data, acquired from the European Marine Observation and Data Network [32] at a 1/16 arc sec resolution, was utilised, and a 2D interpolation using Scipy's RectBivariateSpline function was employed to project this data onto the nodes of the unstructured mesh. The resulting bathymetry plot over the domain is illustrated in Fig. 2.

To get a reliable signal at the Dutch coast line all models were run for a 52 day period, which included a 14 day spinup, a 7 day clean week of signals and a 31 day simulation period. Due to data availability for validations, models were run from June 24th 2016 00:00 till August 15th 2016 00:00, with 1800 s export times.

2.3. MSL scenario

This study examines Mean Sea Level (MSL) rise its impact on tidal energy potential along the Dutch coast, emphasising a robust analysis of MSL changes. Utilising both tide gauge and satellite data, MSL estimates are obtained. Tide gauges offer a historical perspective from 1880 to 2021, with data obtained from Permanent Service for Mean Sea Level (PSMSL) [33], revealing varying MSL rise gradients along the coast, as shown in Fig. 3. A super-linear growth trend is observed, with average yearly increases of 1.89 mm/year (1880–2021) and 3.07 mm/year (1993–2021) over all tide gauge stations on average. Satellite data from 1993 to 2022 indicates a yearly rise of 3.18 mm. To set a single MSL increase rate over the domain, the increase rates from 1993 till 2021 from Harlingen (3.86 mm/year) and Vlissingen (3.09 mm/year) are averaged out and yield a 2050 MSL rise scenario of 3.48 mm/year ending up with a 118 mm increase in 2050, aligning with KNMI scenarios [34]. As super-linear growth is suggested this is a conservative increase forecast in expected MSL rise and is applied to all 2050 THETIS models.

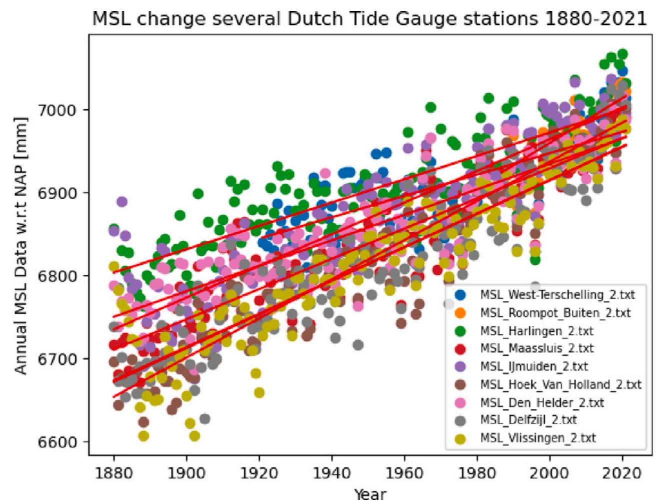

Fig. 3. Linear analysis on tide gauge stations along the Dutch coast, and curve fitting to determine expected changes.

2.4. Models run

Five model runs are executed, comprising two 2016 models, representing summer and winter, and three 2050 models, including summer and winter models and a summer model with additional long-term constituents. As the summer and winter models show very similar outcomes (expected as atmospheric pressure and wind stress are not taken into account), only the summer models are further considered in this research. The inclusion of the specific constituents aims to explore their influence, which has been earlier described by Heigh et al. 2011 [35], on tides and potentially energy density, particularly in the timescale context of the MSL rise scenario applied in this research. This involves two long-period constituents, Mf and Mm and three nonlinear harmonic constituents, M4, MS4, and MN4.

In addition, the depth shift is applied to the 2050 models to account for MSL rise. From all models, the velocity (m/s), elevation (m) and energy density fields (W/m^2) are extracted. With the energy density field as a measure on how many watts of energy are available in a vertical water column (depth averaged) per square metre. Which is quantified as:

$$\text{Energy density flux} = \frac{P}{A} = \frac{1}{2}\rho U^3 \ [\text{W/m}^2] \tag{4}$$

Since all models are run on exactly the same mesh, the elevation, velocity and energy density fields are directly subtracted from each other to provide insight into the differences. Visualisations of the output are constructed using ParaView [36]. To evaluate changes in future tidal stream potential due to MSL rise, the 2016 summer model is considered first. After which the 2050 summer models can be directly compared to the 2016 scenarios. From this a conclusion can be drawn on whether and how MSL rise changes tidal stream potential along the Dutch coast towards 2050.

3. Results

3.1. Model validation

To assess the base model's accuracy, the simulated elevation data from selected tide gauge stations, shown in Fig. 4, were compared with real-time observations obtained from the Copernicus Marine Service Information [37]. The commonly used metric Root Mean Square Error (RMSE), provides a measure of the average difference between the

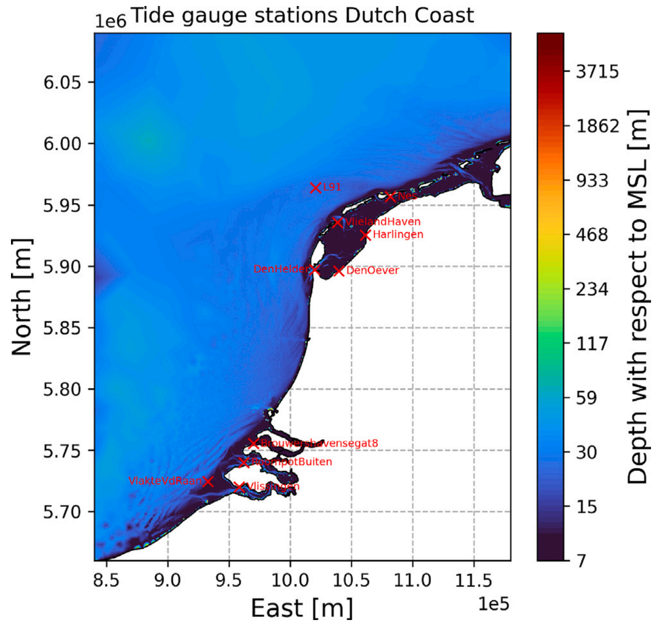

Fig. 4. Tide gauge stations locations in the Dutch coastlines.

Table 1
Comparison between RMSE with harmonic analysis data and real time observations.

	RMSE obs vs. sim	RMSE anal vs. sim	Accuracy increase
Den Helder	0.17 m	0.12 m	29%
Harlingen	0.35 m	0.29 m	17%
Vlakte Vd Raan	0.44 m	0.43 m	2%
L91	0.18 m	0.13 m	28%
Nes	0.32 m	0.27 m	16%
Vlieland Haven	0.21 m	0.17 m	19%
Den Oever	0.18 m	0.11 m	39%
Vlissingen	0.48 m	0.47 m	2%
Roompot Buiten	0.40 m	0.39 m	3%
Brouwersgat	0.35 m	0.34 m	3%

simulated and observed elevation values, is utilised. The RMSE is calculated using the following equation:

$$RMSE = \sqrt{\frac{1}{N}\sum_{i=1}^{N}\left(y_i - \hat{y}_i\right)^2} \tag{5}$$

In which **N** represents the number of data points, y_i is the observed elevation value, and $\hat{y}$ is the simulated elevation value at the ith data point. By taking the square root of the average of the squared differences, RMSE provides a comprehensive measure of the overall accuracy of the model. In addition the coefficient of determination and the scatter index are used to further analyse the data.

At the Wadden Sea, the model exhibited good phase alignment, but some discrepancies were noted at peak signals, potentially influenced by atmospheric pressure and wind stress, as they were not taken into account and particularly present due to the open expanse of the Wadden Sea. The validation for the coast in Zeeland revealed a strong determination coefficient ($r^2 = 0.98$), yet slight deviations from the 1:1 line indicated damping effects, possibly linked to the Manning value. To increase the model's validity, two methods were executed.

First, a new signal was created with a harmonic analysis on the real time observation data, using the Uptide package [38] on the used constituents (M2, S2, K1, O1, P1, Q1, N2, K2), to mitigate the impact of atmospheric pressure and wind stress on elevation measurements. Improving accuracy significantly, especially in the Wadden Sea, as found in Table 1.

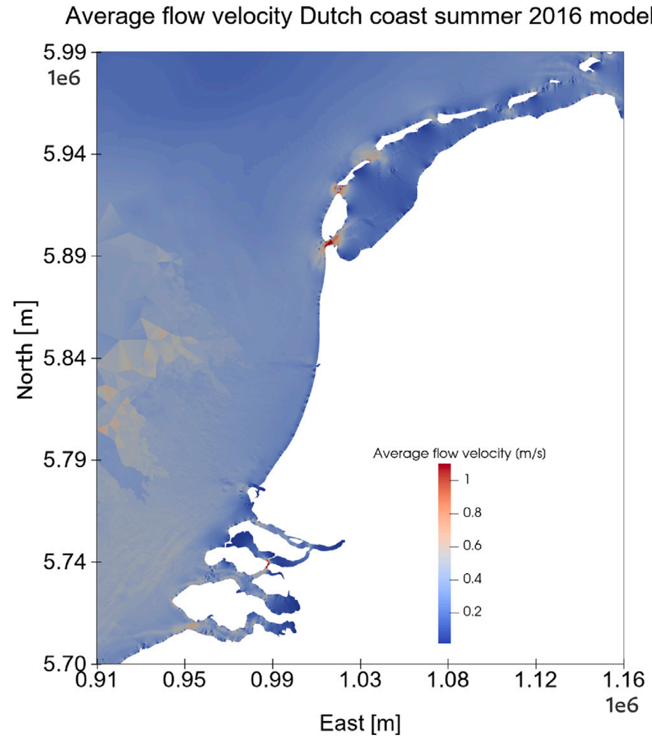

Fig. 5. Average flow velocities 2016 summer model Dutch coast.

Table 2
Average RMSE comparison Manning values.

	RMSE	RMSE Wadden	RMSE Zeeland
Manning 0.05	0.44 m	0.30 m	0.66 m
Manning 0.045	0.39 m	0.26 m	0.59 m
Manning 0.04	0.34 m	0.22 m	0.53 m
Manning 0.035	0.27 m	0.18 m	0.41 m
Manning 0.03	0.24 m	0.20 m	0.31 m

Subsequently, a sensitivity analysis is performed on the Manning value to address potential damping effects within the model, especially for the area around Zeeland. The sensitivity analysis involves testing five Manning values ranging from 0.03 to 0.05 in increments of 0.005. The results, detailed in Table 2, reveal that Manning 0.03 produces the lowest average RMSE (0.24 m). Notably, in Zeeland, Manning 0.03 provides the most favourable outcomes, while for the Wadden Sea, Manning 0.035 is recommended. This optimal Manning value of 0.03 will be utilised in the subsequent phases of this research to determine energy density for the years 2016 and 2050.

3.2. THETIS 2016 tidal stream model

The 2016 summer model average speed plots suggests moderate flow velocities for tidal energy extraction in the Dutch coastal areas the Netherlands, as shown in Fig. 5. Maximum average flow velocities within the Netherlands are obtained in the Wadden Sea and Zeeland, which is in line with Alday and Lavidas (2024) [15].

Looking at the Wadden Sea specifically, highest flow velocities occur between Texel and the main land, where average flow velocities of 1.1 to 1.3 m/s are observed. Following that is the entrance between Texel and Vlieland, where average current speeds of 0.8–1.0 m/s are occurring. And finally, two more spots where +0.5 m/s average speeds have been identified, between Vlieland and Terschelling (0.6–0.8 m/s) and between Terschelling and Ameland (0.6–0.7 m/s). All of which are enlarged in Fig. 6.

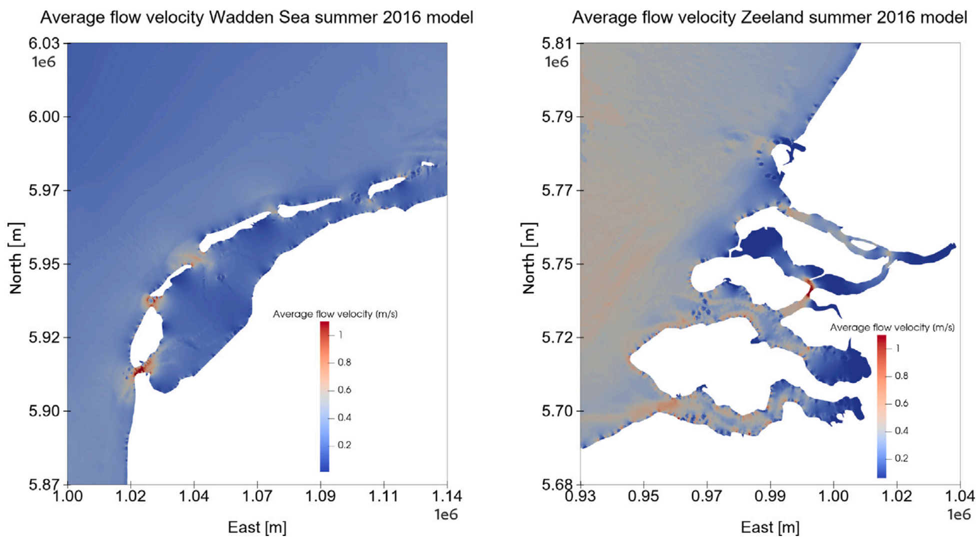

Fig. 6. Average flow velocities 2016 summer model Wadden Sea (left panel) & Zeeland (right panel).

For Zeeland, only the Westerschelde is assumed as a potential area for tidal energy, as the rest of Zeeland's water bodies are controlled by water works which are not taken into account in the models. This means that only this part of Zeeland is considered in this study. Looking at its average flow velocities, as shown in Fig. 6, highest values are obtained at the very beginning of the Westerschelde, near Vlissingen. Where average flow velocities of 0.6–0.75 m/s are observed. Apart from this, no other places with constant average flow velocities of over 0.5 m/s are identified.

Looking at maximum speeds, speeds of 2.0–2.4 m/s are seen in the Wadden Sea between Texel and the mainland. Maximum speeds of 1.3–1.7 m/s between Texel and Vlieland, 1.3–1.6 m/s between Vlieland and Terschelling and 1.3–1.6 m/s between Terschelling and Ameland. In terms of both average and maximum current speeds and the area over which they extend, the area between Texel and the mainland shows thus relatively the highest tidal potential. The maximum speeds obtained near Vlissingen are of magnitude 1.3–1.45 m/s. The energy density field along the Dutch coast for the 2016 model is shown in Fig. 7.

Zooming in on the previously indicated areas in the Wadden Sea and Zeeland, average energy densities of 1200–1600 W/m^2 are observed in the Wadden Sea between Texel and the mainland. As well as 300–600 W/m^2 between Texel and Vlieland, 300–350 W/m^2 between Vlieland and Terschelling and 200–300 W/m^2 between Terschelling and Ameland. In Zeeland, average energy densities of 200–300 W/m^2 are observed for the area near Vlissingen as shown in Fig. 7.

In terms of maximum obtained energy densities, Fig. 8 suggests values of 4000–7000 W/m^2 for between Texel and the mainland, about 1000–2300 W/m^2 between Texel and Vlieland, about 1000–2000 W/m^2 between Vlieland and Terschelling and about 1000–2000 W/m^2 between Terschelling and Ameland. For Vlissingen maximum values of 1200–1600 W/m^2 are observed. The 2016 summer model output confirms previous research by Alday and Lavidas (2024) [15] on Dutch tidal potential, to have low resource areas along its coast located in the Wadden sea and Zeeland.

3.3. Tidal stream differences between 2050 and 2016

Since no difference between winter and summer is assumed, conclusions on how tidal stream energy resources along the Dutch coast are affected by MSL rise (+118.15 mm) will follow directly from the results of the comparison between summer 2050 and summer 2016. The average flow velocity fields, maximum flow velocity fields, average energy density fields and maximum energy density fields were directly subtracted from each other (summer 2050 - summer 2016), in order to effectively orchestrate possible changes. Focusing on the earlier described potential tidal stream areas in the Wadden Sea and Zeeland (Fig. 9), it can be observed that differences for average flow velocities are in a range of 0–0.015 m/s, which is very low, indicating no clear changes towards 2050. When examining the differences in maximum flow velocities (Fig. 10), slightly higher values are obtained, +0.05 to +0.08 m/s near Vlissingen and +0.05 to +0.065 m/s between Texel and the main land. Smaller differences are obtained in the other areas in the Wadden Sea; +0.02 to +0.05 m/s between Texel and Vlieland, +0.03 to +0.05 m/s between Vlieland and Terschelling and +0.04 to +0.06 m/s between Terschelling Ameland. When converting this to energy density, very little changes are seen on average (Fig. 11). Maximum increases of 25 W/m^2 are observed for the average energy density between Texel and the mainland, for the rest, no changes above 10 W/m^2 exist in the Wadden Sea. For the area in the Westerschelde near Vlissingen, maximum changes in average energy density changes are not larger than 8 W/m^2. From which it can be concluded that, on average, no significant changes are expected in tidal stream resources along the Dutch coast. Fig. 12 shows how 2050 would differ from 2016 in term of maximum energy density. Maximum changes of 450 W/m^2 are observed between Texel and the mainland, and maximum changes of no more than 250 W/m^2 are observed at the other sites in the Wadden Sea. For the area near Vlissingen increases not larger then 200 W/m^2 are observed.

3.4. 2050 summer with additional long term constituents vs. 2050 summer without

To ensure that there is a clear understanding of the extent to which long-term constituents could play a role in tidal stream potential, the initial summer 2050 model is compared to the summer 2050 model with additional long term constituents taken into account. To do so, the differences between average velocity fields are examined (2050 summer with long term constituents - 2050 summer), as shown in Fig. 13. As differences in average flow velocities are very close to zero (maximum 0.003 m/s), it is clear both the differences in average flow velocity and the differences in energy density are nil. It therefore follows that the tidal stream potential is not noticeably affected by the addition of long-term constituents to the tidal forcing of the model.

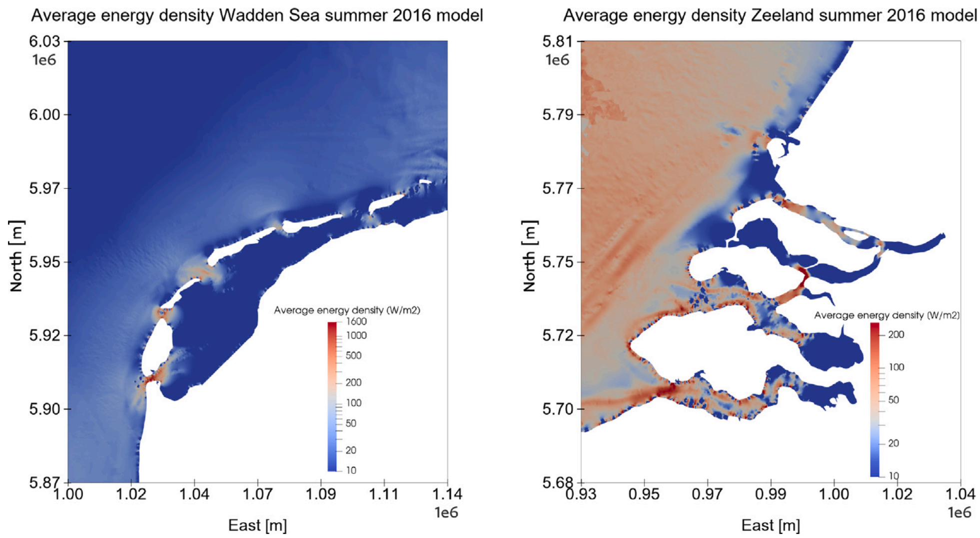

Fig. 7. Average energy density model summer 2016, Wadden Sea (left panel) and Zeeland (right panel).

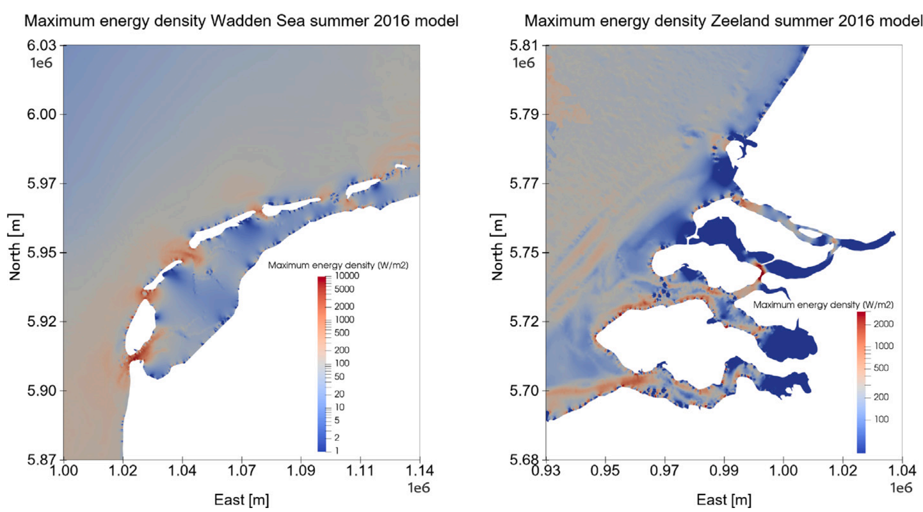

Fig. 8. Maximum energy density model summer 2016, Wadden Sea (left panel) and Zeeland (right panel).

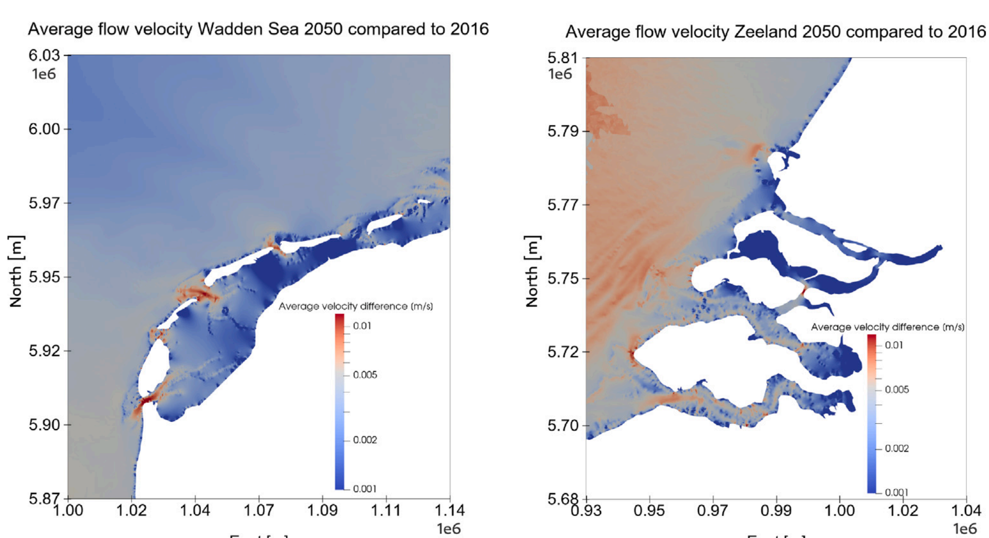

Fig. 9. Average velocity field summer 2016 subtracted from summer 2050, Wadden Sea (left panel) and Zeeland (right panel).

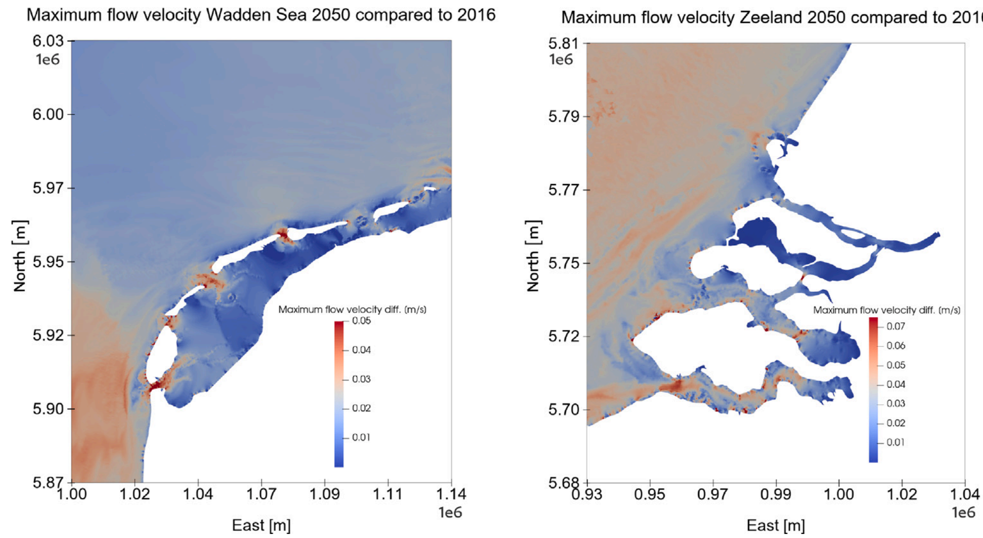

Fig. 10. Maximum velocity field summer 2016 subtracted from summer 2050, Wadden Sea (left panel) and Zeeland (right panel).

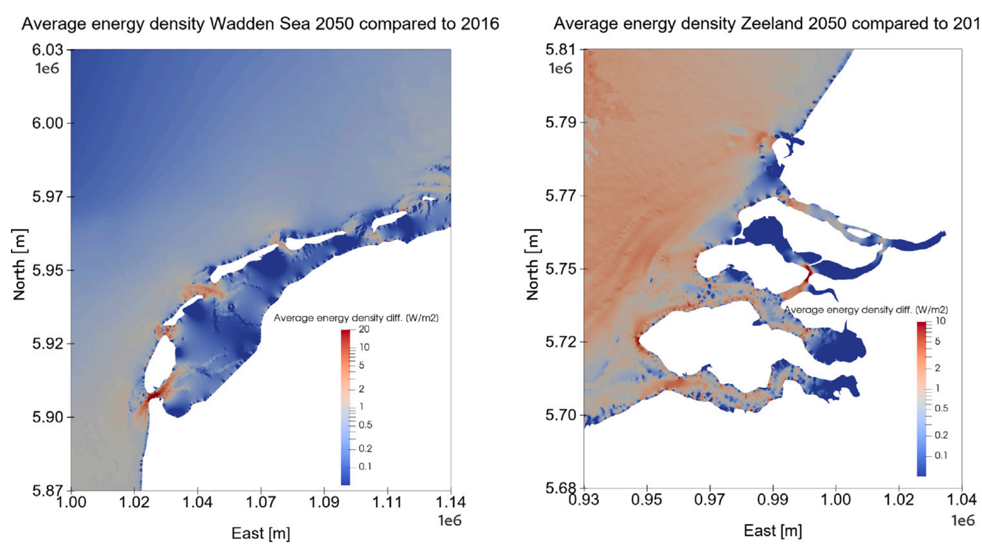

Fig. 11. Energy density field summer 2016 subtracted from summer 2050, Wadden Sea (left panel) and Zeeland (right panel).

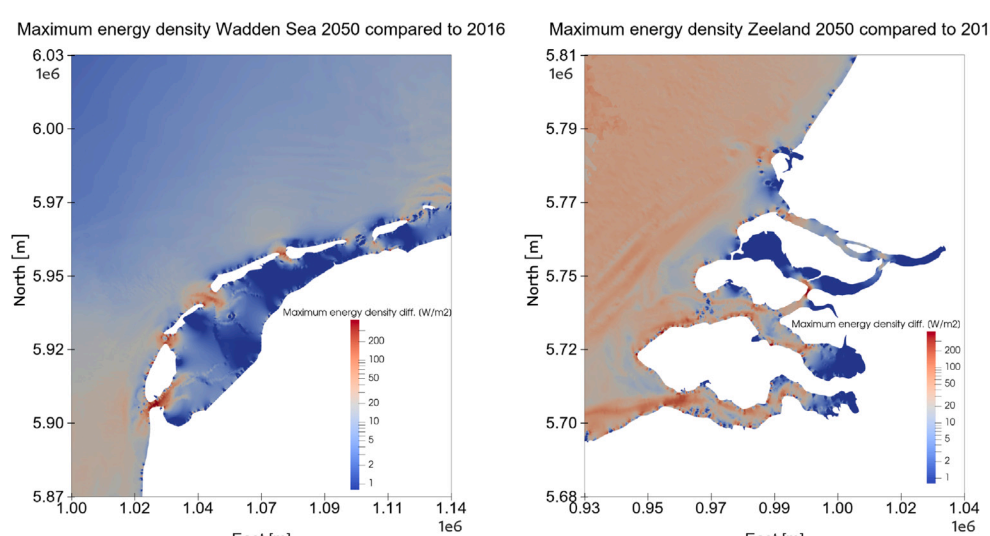

Fig. 12. Maximum energy density field summer 2016 subtracted from summer 2050, Wadden Sea (left panel) and Zeeland (right panel).

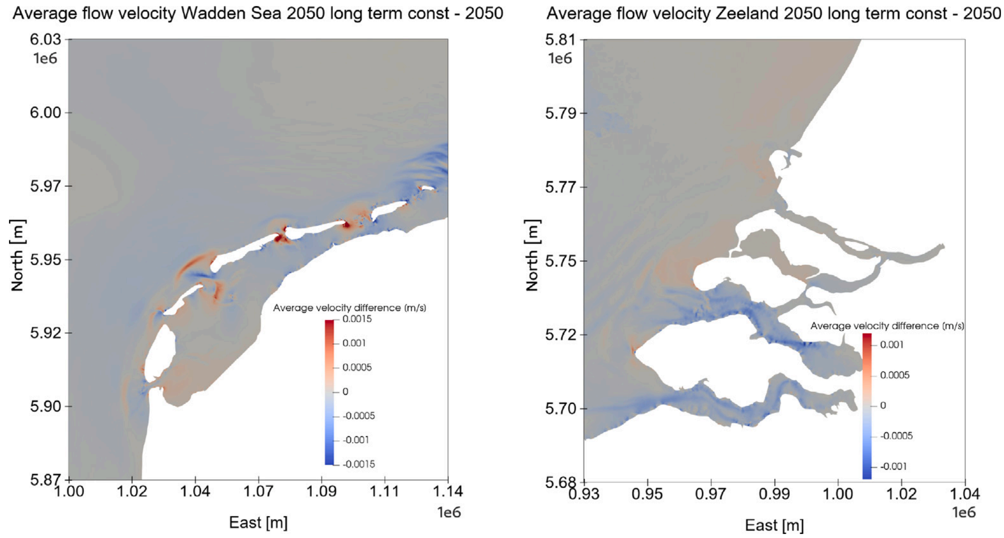

Fig. 13. Average flow velocity field summer 2050 subtracted from summer 2050 with long term constituents, Wadden Sea (left panel) and Zeeland (right panel).

4. Discussion

This research focuses on the tidal stream resource change over time primarily. Changes are therefore rather examined over extended periods (using the average energy density fields) than targeting short bursts of high energy density (maximum energy density fields). It can be concluded that no clear changes in tidal stream resources are observed due to MSL rise along the Dutch coast towards 2050. Tidal stream resources consequently can be assumed to remain constant towards 2050 even given proposed MSL rise.

In addition, the low velocities also suggest that smaller diameter tidal turbines will be more beneficial, in order to maximise energy extraction. Such smaller diameter devices may also benefit by advancements in 3D printed elements that can reduce the deployment time. However, this research was not interested in evaluating tidal stream arrays or their positioning, therefore the economic feasibility would require a different approach [39]. The findings, can securely indicate that the designs selected for the Netherlands will be expected to produce reliability for the decades to come, even with the impacts of Climate Change on the tidal resource.

The hot-spot areas for tidal stream are located in the North and South of the country where the expected contribution can be vastly different. In the North, tidal stream has higher mean and maxima values, whilst at the same time the Wadden islands have a weaker grid connectivity to the mainland, and are actively seeking to decarbonise. In the southern regions the connectivity is higher and nearby the port of Rotterdam and other industrial hubs can benefit by the tidal predicability. The findings of this study can be used by the Dutch government and other stakeholders involved in shaping the future energy landscape of the Netherlands, with the goal of enhancing the utilisation of indigenous renewable energy resources.

5. Conclusion

This study assessed the resource potential for tidal stream energy in the Netherlands, taking also into account changes in potentials due to MSL rise towards 2050. Despite being a low resource area, this study suggests that the tidal resource will not be affected by Climate Change. Analysis of historical data over the past decade has highlighted varying rates of mean sea level (MSL) rise along the Dutch coast, ultimately resulting in an estimated average increase of 3.475 mm per year towards 2050. Considering this trend, it is projected that the Netherlands may experience a total MSL rise of 118.15 mm from 2016 to 2050.

The base model for 2016 (using a 0.035 Manning value) showed satisfactory validation (RMSE's ranging from 0.17 to 0.44 m) when compared to real-time observations at tide gauges across the country. However, some observations could not be explained by the model simulation due to irregularities likely caused by atmospheric pressure and wind stress. Particularly in the Wadden Sea, which is more exposed to open sea conditions, irregularities were perceived in the observation data, and to a lesser extent in Zeeland, characterised by an estuary environment.

The validation of the improved tidal model confirmed its reliability and suitability as a base model for 2016 and 2050. Subsequently, five models were run to analyse the effects of MSL rise on the tidal stream potential towards 2050. Comparison between the 2016 summer and winter models indicated similar outputs, so that the summer models for both 2016 and 2050 were representative.

The results of the 2016 summer model revealed low tidal energy resources in the Netherlands generally. However in the Wadden Sea the area between Texel and the mainland exhibited average flow velocities of 1.1 to 1.3 m/s and energy densities of 1200–1600 W/m^2, while in Zeeland the Westerschelde showed its highest potential at its inlet with flow velocities of 0.6–0.75 m/s and energy densities of 200–300 W/m^2. These findings suggest the possibility of utilising downscaled tidal stream turbines in these regions, despite the overall low resource availability compared to other sites in for instance the UK and France which have resources significantly higher, that have tidal stream velocities of $\geq$3.5 m/s.

Analysing the differences between the 2050 and 2016 models, minor variations in average velocities (0–0.015 m/s) and average energy density (up to 25 W/m^2) were observed. As these differences were not significant it indicates that tidal stream resources are unlikely to be affected by MSL rise scenarios towards 2050. Finally, when examining the inclusion of long-term constituents in the model, it was found that their incorporation did not significantly impact the results for 2050 compared to the regular 2050 summer model, with maximum average velocity differences of 0.003 m/s.

CRediT authorship contribution statement

Sijbrand Bolhuis: Writing – original draft, Visualization, Validation, Methodology, Data curation, Conceptualization. **Matias Alday:** Writing – review & editing, Supervision, Conceptualization. **George Lavidas:** Writing – review & editing, Supervision, Conceptualization.

Declaration of competing interest

All authors declare that they have no known competing financial interests or personal relationships that could have appeared to influence the work reported in this paper.

Acknowledgements

The authors express their gratitude to Tuomas Kärnä, Jon Hill, and Joe Wallwork for their ongoing assistance in implementing Thetis, mesh generation, and engaging discussions. Special appreciation goes to Dennis Palagin for facilitating the installation of Thetis in the Delft-Blue HPC. Lastly, the authors appreciate the anonymous reviewers whose valuable comments and suggestions played an important role in shaping the final version of this study.

References

[1] S.P. Neill, A. Vögler, A.J. Goward-Brown, S. Baston, M.J. Lewis, P.A. Gillibrand, S. Waldman, D.K. Woolf, The wave and tidal resource of Scotland, Renew. Energy 114 (2017) 3–17, http://dx.doi.org/10.1016/J.RENENE.2017.03.027.

[2] M. Lewis, J. McNaughton, C. Márquez-Dominguez, G. Todeschini, M. Togneri, I. Masters, M. Allmark, T. Stallard, S. Neill, A. Goward-Brown, P. Robins, Power variability of tidal-stream energy and implications for electricity supply, Energy 183 (2019) 1061–1074, http://dx.doi.org/10.1016/J.ENERGY.2019.06.181.

[3] N. Guillou, S.P. Neill, J. Thiébot, Spatio-temporal variability of tidal-stream energy in north-western Europe, Phil. Trans. R. Soc. A 378 (2178) (2020) 20190493.

[4] S.C. Warder, A. Angeloudis, M.D. Piggott, Sedimentological data-driven bottom friction parameter estimation in modelling Bristol channel tidal dynamics, Ocean. Dyn. 72 (6) (2022) 361–382.

[5] N. Guillou, S.P. Neill, P.E. Robins, Characterising the tidal stream power resource around France using a high-resolution harmonic database, Renew. Energy 123 (2018) 706–718, http://dx.doi.org/10.1016/J.RENENE.2017.12.033.

[6] Z. Yang, T. Wang, R. Branch, Z. Xiao, M. Deb, Tidal stream energy resource characterization in the Salish sea, Renew. Energy 172 (2021) 188–208, http://dx.doi.org/10.1016/J.RENENE.2021.03.028.

[7] P. Gao, J. Zheng, J. Zhang, T. Zhang, Potential assessment of tidal stream energy around Hulu Island, China, Procedia Eng. 116 (1) (2015) 871–879, http://dx.doi.org/10.1016/J.PROENG.2015.08.376.

[8] S.P. Neill, M. Hemmer, P.E. Robins, A. Griffiths, A. Furnish, A. Angeloudis, Tidal range resource of Australia, Renew. Energy 170 (2021) 683–692, http://dx.doi.org/10.1016/J.RENENE.2021.02.035.

[9] K. Orhan, R. Mayerle, W.W. Pandoe, Assesment of energy production potential from tidal stream currents in Indonesia, Energy Procedia 76 (2015) 7–16, http://dx.doi.org/10.1016/J.EGYPRO.2015.07.834.

[10] D. Coles, A. Angeloudis, D. Greaves, G. Hastie, M. Lewis, L. Mackie, J. McNaughton, J. Miles, S. Neill, M. Piggott, others, A review of the UK and British channel Islands practical tidal stream energy resource, Proc. R. Soc. A 477 (2255) (2021) 20210469.

[11] D. Wesselman, R. de Winter, A. Engelstad, R. McCall, A. van Dongeren, P. Hoekstra, A. Oost, M. van der Vegt, The effect of tides and storms on the sediment transport across a dutch barrier Island, Earth Surf. Process. Landf. 43 (3) (2018) 579–592.

[12] L. Jiang, T. Gerkema, D. Idier, A.B.A. Slangen, K. Soetaert, Effects of sea-level rise on tides and sediment dynamics in a Dutch tidal bay, Ocean. Sci. 16 (2) (2020) 307–321, http://dx.doi.org/10.5194/os-16-307-2020, URL https://os.copernicus.org/articles/16/307/2020/.

[13] A. de Fockert, A.C. Bijlsma, T.S.D. O'Mahoney, W. Verbruggen, P.C. Scheijgrond, Z.B. Wang, Assessment of the impact of tidal power extraction from the eastern Scheldt storm surge barrier through the evaluation of a pilot plant, Renew. Energy 213 (2023) 109–120, http://dx.doi.org/10.1016/J.RENENE.2023.06.001.

[14] T. O'Mahoney, A. de Fockert, A.C. Bijlsma, P. de Haas, Hydrodynamic impact and power production of tidal turbines in a storm surge barrier, Int. Mar. Energy J. 3 (3) (2020) 127–136.

[15] M. Alday, G. Lavidas, Assessing the tidal stream resource for energy extraction in The Netherlands, Renew. Energy 220 (2024) 119683, http://dx.doi.org/10.1016/J.RENENE.2023.119683.

[16] J. van Alphen, M. Haasnoot, F. Diermanse, Uncertain accelerated sea-level rise, potential consequences, and adaptive strategies in The Netherlands, Water 14 (10) (2022) http://dx.doi.org/10.3390/w14101527, URL https://www.mdpi.com/2073-4441/14/10/1527.

[17] D. Idier, F. Paris, G.L. Cozannet, F. Boulahya, F. Dumas, Sea-level rise impacts on the tides of the European shelf, Cont. Shelf Res. 137 (2017) 56–71, http://dx.doi.org/10.1016/J.CSR.2017.01.007.

[18] B. Kresning, M.R. Hashemi, S.P. Neill, J.A.M. Green, H. Xue, The impacts of tidal energy development and sea-level rise in the Gulf of Maine, Energy 187 (2019) 115942, http://dx.doi.org/10.1016/j.energy.2019.115942, URL https://www.sciencedirect.com/science/article/pii/S0360544219316263.

[19] T. Kärnä, V. Legat, E. Deleersnijder, H. Burchard, Coupling of a discontinuous Galerkin finite element marine model with a finite difference turbulence closure model, Ocean. Model. 47 (2012) 55–64, http://dx.doi.org/10.1016/J.OCEMOD.2012.01.001.

[20] A. Angeloudis, S.C. Kramer, N. Hawkins, M.D. Piggott, On the potential of linked-basin tidal power plants: An operational and coastal modelling assessment, Renew. Energy 155 (2020) 876–888, http://dx.doi.org/10.1016/J.RENENE.2020.03.167.

[21] A. Angeloudis, S.C. Kramer, A. Avdis, M.D. Piggott, Optimising tidal range power plant operation, Appl. Energy 212 (2018) 680–690, http://dx.doi.org/10.1016/j.apenergy.2017.12.052.

[22] F. Rathgeber, D.A. Ham, L. Mitchell, M. Lange, F. Luporini, A.T.T. Mcrae, G.-T. Bercea, G.R. Markall, P.H.J. Kelly, .D.A. Ham, .P.H.J. Kelly, Firedrake: Automating the finite element method by composing abstractions, ACM Trans. Math. Software 43 (3) (2016) 24, http://dx.doi.org/10.1145/2998441.

[23] S. Balay, S. Abhyankar, M. Adams, J. Brown, P. Brune, K. Buschelman, L. Dalcin, A. Dener, V. Eijkhout, W. Gropp, others, PETSc users manual, 2019.

[24] M.R. Hestenes, E. Stiefel, others, Methods of conjugate gradients for solving linear systems, J. Res. Natl. Bur. Stand. 49 (6) (1952) 409–436.

[25] U.M. Ascher, S.J. Ruuth, R.J. Spiteri, Implicit-explicit Runge-Kutta methods for time-dependent partial differential equations, Appl. Numer. Math. 25 (2) (1997) 151–167, http://dx.doi.org/10.1016/S0168-9274(97)00056-1, URL https://www.sciencedirect.com/science/article/pii/S0168927497000561.

[26] E.E. Mawson, K.C. Lee, J. Hill, Sea level rise and the Great Barrier Reef the future implications on reef tidal dynamics, J. Geophys. Res. Ocean. (2022) e2021JC017823.

[27] G.D. Egbert, S.Y. Erofeeva, Efficient inverse modeling of barotropic ocean tides, 2002.

[28] A. Avdis, A.S. Candy, J. Hill, S.C. Kramer, M.D. Piggott, Efficient unstructured mesh generation for marine renewable energy applications, Renew. Energy 116 (2018) 842–856, http://dx.doi.org/10.1016/J.RENENE.2017.09.058.

[29] C. Geuzaine, J.F. Remacle, Gmsh: A 3-D finite element mesh generator with built-in pre- and post-processing facilities, Internat. J. Numer. Methods Engrg. 79 (11) (2009) 1309–1331, http://dx.doi.org/10.1002/nme.2579.

[30] P. Wessel, W.H.F. Smith, A global, self-consistent, hierarchical, high-resolution shoreline database, J. Geophys. Res. Solid Earth 101 (B4) (1996) 8741–8743, http://dx.doi.org/10.1029/96JB00104, URL https://agupubs.onlinelibrary.wiley.com/doi/abs/10.1029/96JB00104.

[31] QGIS Geographic Information System, QGIS.org, 2020, URL http://www.qgis.org.

[32] E.B. Consortium, others, Emodnet digital bathymetry (dtm 2016), 2016.

[33] S.J. Holgate, A. Matthews, P.L. Woodworth, L.J. Rickards, M.E. Tamisiea, E. Bradshaw, P.R. Foden, K.M. Gordon, S. Jevrejeva, J. Pugh, New data systems and products at the permanent service for mean sea level, J. Coast. Res. 29 (3) (2013) 493–504.

[34] B. Van Den Hurk, P. Siegmund, A. Klein Tank, KNMI'14: Climate change scenarios for the 21st Century-A Netherlands perspective, 2014, URL www.climatescenarios.nl.

[35] I.D. Haigh, M. Eliot, C. Pattiaratchi, Global influences of the 18.61 year nodal cycle and 8.85 year cycle of lunar perigee on high tidal levels, J. Geophys. Res. Ocean. 116 (6) (2011) http://dx.doi.org/10.1029/2010JC006645.

[36] A.H. Squillacote, J. Ahrens, C. Law, B. Geveci, K. Moreland, B. King, The Paraview Guide, Vol. 366, Kitware Clifton Park, NY, 2007.

[37] E.U. Copernicus Marine Service Information, Atlantic-European north west shelf-ocean in-situ near real time observations, 2023, http://dx.doi.org/10.48670/moi-00045.

[38] S. Kramer, T. Kärnä, J. Hill, S.W. Funke, Stephankramer/uptide: First release of uptide v1. 0, 2020.

[39] H. Gonabadi, S.F. Hosseini, Y. Chen, S. Bull, Structural analysis of small-scale 3D printed composite tidal turbine blades, Ocean Eng. 306 (2024) 118057, http://dx.doi.org/10.1016/j.oceaneng.2024.118057, URL https://www.sciencedirect.com/science/article/pii/S0029801824013957.